

# Finite-element method for intermodality nonrigid breast registration using external skin markers

Ioana L. Coman<sup>\* 1,2,4</sup>, Andrzej Krol<sup>2,4,6</sup>, James A. Mandel<sup>3</sup>, Karl G. Baum<sup>4</sup>, Min Luo<sup>5</sup>,  
Edward D. Lipson<sup>6,2,4</sup>, David H. Feiglin<sup>2</sup>

<sup>1</sup>Department of Mathematics and Computer Science, Ithaca College

<sup>2</sup>Department of Radiology, SUNY Upstate Medical University

<sup>3</sup>Department of Civil and Environmental Engineering, Syracuse University

<sup>4</sup>Department of Electrical Engineering and Computer Science, Syracuse University

<sup>5</sup>Department of Biomedical Engineering, University of Wisconsin-Madison

<sup>6</sup>Department of Physics, Syracuse University

## ABSTRACT

We are developing a method using nonrigid co-registration of PET and MR breast images as a way to improve diagnostic specificity in difficult-to-interpret mammograms, and ultimately to avoid biopsy. A deformable breast model based on a finite-element method (FEM) has been employed. The FEM "loads" are taken as the observed intermodality displacements of several fiducial skin markers placed on the breast and visible in PET and MRI. The analogy between orthogonal components of the displacement field and the temperature differences in a steady-state heat transfer (SSHT) in solids has been adopted. The model allows estimation, throughout the breast, of the intermodality displacement field. To test our model, an elastic breast phantom with simulated internal "lesions" and external markers was imaged with PET and MRI. We have estimated fiducial- and target-registration errors vs. number and location of fiducials, and have shown that the SSHT approach using external fiducial markers is accurate to within ~5 mm.

**Keywords:** Nonrigid registration, finite element method, multimodality imaging

## 1. INTRODUCTION

Breast cancer is the most common malignant disease in women, and the second leading cause of cancer death among American women today [1]. One of the major goals in breast-cancer diagnosis is early detection. The primary tool for detection and diagnosis of breast cancer is x-ray mammography. The normal follow-up diagnostic treatment after equivocal or difficult-to-interpret screening mammography is surgical biopsy. Since the majority of breast biopsies turn out negative [3], it would be highly desirable to have an alternative, noninvasive approach as the second line of defense after mammography. Accordingly, we have begun experimenting with intermodality (PET and MRI) nonrigid breast-image co-registration, using a 3D FEM-based deformable breast model. This model estimates the displacement field for any location in the breast, using observed displacements of external fiducial markers visible in both PET and MRI images.

## 2. MATERIALS AND METHODS

For our experiments we used a custom-manufactured deformable breast phantom (CIRS Inc., Norfolk, VA; [www.cirsinc.com](http://www.cirsinc.com)), filled with medium-stiffness gel (vinyl-based hydrolymer with low concentration of nickel chloride) and surrounded by a skin made of thin urethane foil (Fig. 1).

The phantom was imaged using F-18-FDG positron emission tomography (PET) and high-resolution magnetic resonance imaging (MRI). Table I shows the scan details.

---

\* [ilcoman@ecs.syr.edu](mailto:ilcoman@ecs.syr.edu); <http://web.syr.edu/~ilcoman>; tel. 607-274-5704

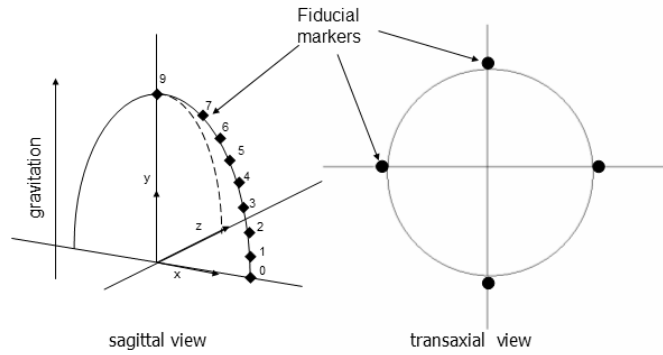
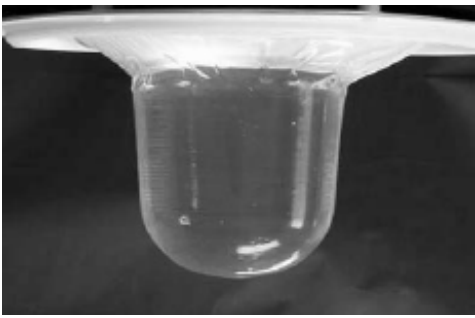


Fig. 1. *Left*: Elastic breast phantom with external fiducial markers. *Right*: Placement of eight markers on each of four meridians and one additional marker at the apex.

TABLE I  
IMAGING SPECIFICATIONS

	MRI	PET
Scanner	Philips 1.5 T, Intera	GE Advance
Scan Parameters	T1-weighted isotropic 3D FFE sequences with flip angle 20°	Transmission scan 3 min Emission scan 5 min
Spatial Resolution	0.7 mm	<7 mm
Acquisition/ Reconstruction matrix	512 × 512	128 × 128
Voxel size	0.7 × 0.7 × 1.12	4.25 × 4.25 × 4.25

Breast “lesions” visible in MRI were emulated by injection of oil (Johnson & Johnson), non-diffusing in the gel, containing a mixture of organic azo dyes. To emulate lesions that would be visible in PET, F-18-FDG, diluted in water-soluble gelatin containing organic dyes, was injected as close as possible to the oil “lesions.” Figure 2 shows the locations of six “lesions” that were identified in both PET and MRI.

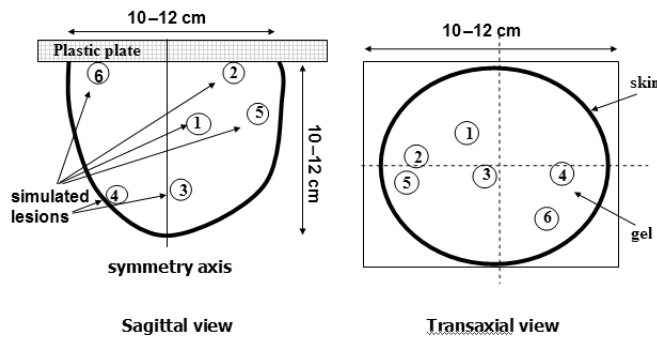


Fig. 2. Locations of “lesions” inside elastic breast phantom detected by PET and MRI.

### 3. MULTIMODALITY CO-REGISTRATION USING DEFORMABLE FEM-BASED MODEL

A deformable, finite-element method (FEM) based model of the elastic breast phantom was constructed [2,4]. Our approach rests on the assumption that stress conditions within the phantom were virtually the same for both modalities. Since the phantom was leveled and freely suspended in PET and MRI, this assumption is justified.

The analogy between orthogonal components of the displacement field and the temperature differences in a steady-state heat transfer (SSHT) in solids was adopted in our deformable FEM-based breast model. The model allows

estimation of the intermodal breast deformation for every location within the breast from observed intermodal displacement of fiducial skin markers that are considered the FEM “loads”. The displacement field components  $u_x$ ,  $u_y$ , and  $u_z$  are mathematically equivalent to temperature differences in the steady-state heat transfer problem, and are all distributed linearly over the phantom domain. Figure 3 shows images of fiducial markers and “lesions” in the elastic breast phantom obtained using PET and MRI.

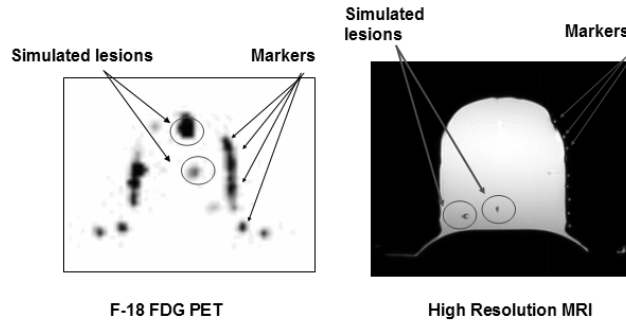


Fig. 3. Representative placement of “lesions” inside deformable breast phantom.

The geometry of the breast was obtained from MRI, and the meshing and FEM analysis were performed using the commercial software package, ANSYS (ver. 5.7, ANSYS Inc., Canonsburg, PA). The following elements were chosen from the ANSYS library: SOLID87 3-D 10-Node Tetrahedral Thermal Solid; SOLID70 3-D Thermal Solid; and SHELL57 2-D Thermal Shell. A mesh containing a total of 15,636 nodes was created (Fig. 4). SOLID87 and SOLID70 elements were used in the bulk of the object. The surface was meshed by a layer of SHELL57 elements.

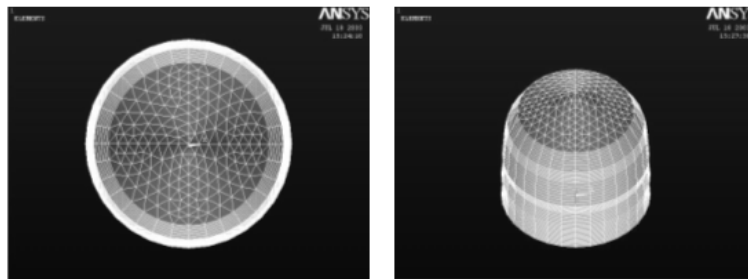


Fig. 4. FEM mesh generated by ANSYS software. *Left*: top view. The outer ring (white) shows shell elements. The inner ring shows brick elements. The central, uppermost area has tetrahedral elements. *Right*: oblique view. Brick elements are visible on the sides, and tetrahedral elements at and near the top.

Thermal conductivity assigned to the surface elements was 1,000 times that used in the bulk of the phantom, in order to assure that the surface layer reaches steady state 1,000 times faster than the interior. Intermodality displacements (between PET and MRI) for every location within the phantom were obtained. The execution time was 20 s per Cartesian component for the entire mesh, using a 3 GHz, dual Xeon processor PC.

#### 4. RESULTS

We estimated two categories of errors: fiducial marker-registration error (FRE), and target-registration error (TRE); see Table II and Fig. 5. FRE was estimated for the fiducial markers that were excluded from the registration process, while TRE was estimated for the internal “lesion”. We have established that the intermodality co-registration—performed on the elastic breast phantom and using our SSHT deformable breast model with external fiducial markers—is accurate to within ~5mm (voxel size in PET). If proximal fiducial markers do not surround the “lesion,” then the TRE can be as large as two PET voxels.

TABLE II  
FIDUCIAL registration errors<sup>1</sup>

No. of markers used in the FEM model	Mean Error (mm)	Standard Deviation (mm)	Min Error (mm)	Max Error (mm)
13	4.06	1.55	2.32	9.94
8	4.27	2.16	1.55	1.55
27 (all)	0.00007	0.00008	0.00002	0.00038

<sup>1</sup>Fiducial registration errors (FRE) were estimated using selected fiducial markers that were not used in the FEM model calculation for PET-MR co-registration. A total of 27 identifiable markers were available.

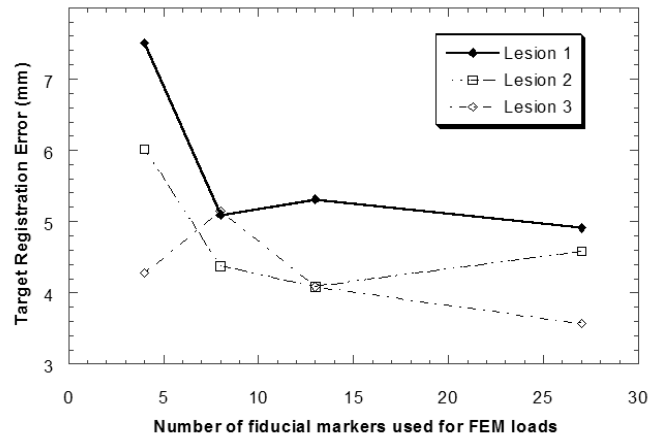


Fig. 5. Dependence of target registration error (TRE) on number of fiducial markers used in steady-state FEM model. Data are shown for three representative “lesions” of the six (see locations, by number, in Fig. 2).

## 5. CONCLUSIONS

The SSHT deformable FEM-based breast model performs well for multimodality elastic breast phantom image co-registration. This co-registration procedure requires that the external fiducial markers surround the suspicious lesion and it requires very careful breast positioning to prevent change in the internal stress condition between different modalities. We plan to investigate the robustness of this approach by intentionally introducing variation in the internal stress conditions in the breast between different modalities and studying the influence of this factor on TRE.

## 6. REFERENCES

1. American Cancer Society (2002). *Cancer Facts and Figures*, <http://www.cancer.org>.
2. *ANSYS Theory Reference* (1999) Eleventh Edition, SAS IP Inc.
3. C. J. Baines (1998). “Menstrual Cycle Variation in Mammographic Breast Density”. *J. Natl. Cancer Inst.*, 90, 875.
4. *The Finite Element Method: Basic Concepts and Applications* (Series in Computational and Physical Processes in Mechanics and Thermal Sciences), Hemisphere Publishing Corporation, 1992.
5. S.L. Sailer, J.G. Rosenman, M. Soltys, T.J. Cullip, J. Chen (1996). “Improving treatment planning accuracy through multimodality imaging,” *Int. J. Radiation Oncology*, 35, 117-124.